Journal of Molecular Structure 1092 (2015) 176–186

Contents lists available at ScienceDirect

Journal of Molecular Structure

journal homepage: www.elsevier.com/locate/molstruc

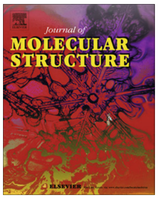

Synthesis, characterization of azobenzene and cinnamate ester based calamitic liquid crystalline compounds and their photoresponsive properties

Chinnaiyan Selvarasu, Palaninathan Kannan *

Department of Chemistry, Anna University, Chennai 600-025, India

HIGHLIGHTS

- Five terminally substituted azobenzene chromophores having azocinnamate as central linkages have been prepared.
- The synthesized liquid crystalline compounds exhibit mesomorphism.
- The effects of morphological modifications on mesophase were studied.
- All the compounds exhibit photoisomerization.

GRAPHICAL ABSTRACT

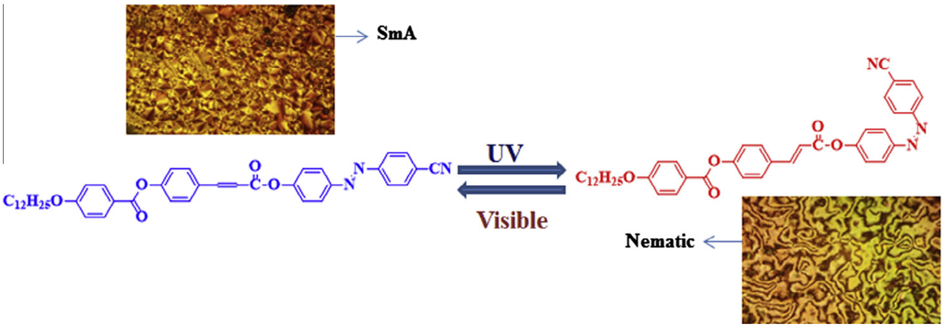

ARTICLE INFO

Article history:
Received 31 October 2014
Received in revised form 20 February 2015
Accepted 17 March 2015
Available online 24 March 2015

Keywords:
Liquid crystals
Thermotropic mesomorphic
Cinnamoyl ester
Trans–cis isomerization
Photochromic compounds

ABSTRACT

A series of azobenzene-containing mesogens end-capped with cinnamoyl esters were synthesized and investigated its mesogenic and photochemical properties. Terminal substituents of the molecules were changed with various substituents like CN, Cl, H, CH_3, and OCH_3. Liquid crystalline properties of the synthesized compounds were studied and confirmed using differential scanning calorimetry, polarising optical microscopy. Compounds (**4a**–**4e**) exhibited a thermotropic mesomorph behaviour viz., nematic and smectic phases that depends on the terminal substituents. The thermal transition temperatures and the mesophase types are depend on the terminal substituents which are ascribed with the increasing cohesive forces between molecules as the conjugation length increases. These photochromic compounds exhibited strong UV–vis absorption maxima between 330 and 340 nm. Upon irradiation with selective UV light produces the trans–cis isomerization producing new maxima at 450 nm due to cis configuration.

Introduction

Liquid crystal mesogens are unique compounds and which find so many applications in the wide spectrum of material chemistry. This is because that they exhibit a number of phases which have not only ordering of crystals but also the molecular mobility of liquid with robust mechanical properties. These self-assembled structures have interesting properties like reversible isomerization, fluorescence emission due to π staking in an orderly state thanks to spacers which gave them the molecular mobility. Liquid crystal compounds are widely used as anisotropic material and they drawn our attention to manipulate high efficiency electro optical devices, holography and reversible optical storage devices [1–3]. On the other hand, azobenzene containing liquid crystal compounds have prospective technological applications such as high density data storage, optical computing, dynamic holography, optical image processing, [4–8] waveguide switches and nonlinear

---

* Corresponding author. Tel.: +91 44 22358666; fax: +91 44 2220 0660.
E-mail address: pakannan@annauniv.edu (P. Kannan).

http://dx.doi.org/10.1016/j.molstruc.2015.03.026
0022-2860/

optical (NLO) materials etc., [9–11] Azobenzene-containing chromophores undergo isomerization from the trans to the cis-isomer upon irradiation by light, whereas the cis isomer can return to the trans form by responding to both light and heat, thus offer many option in photonic applications [12–14]. The study of various types of photoalignment of materials containing cinnamoyl-, coumarin and azobenzene has been already reported [15–17]. Yang et al. studied the photochromic compound, azobenzene substituted chromophores and its optical properties. They synthesized the compounds bearing six or eleven methylene segments which exhibited cholesteric phases and oily streaky texture. And also they introduced the nitro-group in the terminal position which resulted in increased cis to trans-isomerization rates in thermal reversible process [18].

Hence in the present study, we examine the effect of terminal groups and spacer length of chromophores structure on mesomorphic properties. Furthermore, the photoisomerization of these different terminal substituents azobenzene-containing dodecyloxy benzyloxy cinnamic acid and their reversible trans–cis–trans photochemical transformations in chloroform solution were also discussed.

Experimental

Materials and physical measurements

All reagents, starting materials were purchased from Aldrich (Sigma Aldrich, India) and Merck and were used without further purification unless otherwise noted. Thionyl chloride, triethylamine, tetrahydrofuran, dimethlysulfoxide, dimethylformamide, benzene, phenol were performed under dry nitrogen atmosphere. Silica gel 60 (Merck (Darmstadt, Germany)) was used for column chromatography. 4-hydroxybenzoic acid, 4-hydroxycinnamic acid, sodium hydroxide, hydrochloric acid, sodium nitrite, aniline, 4-chloroaniline, 4-methlylaniline, 4-methoxyaniline (Merck, India). Solvents such as tetrahydrofuran (Fisher scientific), dimethylformamide (Merck) were distilled under reduced nitrogen pressure from CaH_2 and subsequently stored over 4 Å molecular sieves. The infrared spectra of the compounds were measured using KBr disk – Perkin Elmer FT-IR spectrometer. ^1H (400 MHz) and ^{13}C NMR (125 MHz) measurements were performed with Bruker spectrometer using TMS as an internal standard. Compositions of the compounds were determined by Heraeus CHN elemental analyser. DSC measurements were performed at a heating rate of 5 °C min^{-1}, and the samples were taken in an aluminium pan with a pierced lid, in a dry nitrogen atmosphere with an empty pan as reference on a TA instrument (model Q 10). The optical texture of compounds were observed using a Euromex polarising optical microscope (POM) equipped with Linkem HFS91 heating stage and TP-93 temperature programmer. Samples were placed in between two thin glass cover slips and melted with heating and cooling at the rate of 1 °C min^{-1}. The photographs were taken with a Canon 1000 D camera. Ultraviolet–visible (UV–vis) absorption measurement and photoisomerization experiment were performed on UV-1650 spectrometer under UV and visible light exposure in the room temperature. The LDBC chloroform solution was prepared with concentration of 1×10^{-5} M, UV irradiation was carried out using 12 W ultraviolet lamp (365 nm), and irradiation by visible light was conducted using a 9 W incandescent lamp (w 420 nm).

Synthetic procedures

Terminally substituted azobenzene **(3a–3e)** were synthesized according to the procedure reported earlier [19] and other precursor 4-(dodecyloxy)benzoic acid was synthesized as per the earlier reports [20] Compounds **4a**–**4e** were synthesized as depicted in Scheme 1. Compound **1** was prepared from alkylated hydroxybenzoic acid converted to acid chloride in the presence of thionyl chloride in benzene. This acid chloride added to 4-hydroxycinnamic acid in the presence of aqueous sodium hydroxide in dimethylsulphoxide to give (E)-3-(4-((4-(dodecyloxy)benzoyl)oxy)phenyl) acrylic acid **(1).** Therein the acid compound **1** was being able to be changed into acid chloride in the presence of thionyl chloride in benzene. Subsequently the acid chloride **2** was reacted with terminally substituted azobenzene **(3a**–**3e)** in the presence of triethylamine in tetrahydrofuran to produce the desired compounds **4a**–**4d.** (4-((E)-3-(4-((E)-(4-cyanophenyl)diazenyl)phenoxy)-3-oxoprop-1-en-1-yl)phenyl 4-(dodecyloxy)benzoate) is **4a** and similar experimental procedures were utilised for the synthesis of other substituents compounds **4b**–**4e** were described in synthesis part. The synthesized compounds were purified using column chromatography (hexane:ethylacetate) and further purified by repeated recrystallization using methanol. All the compounds were subjected to usual spectral techniques to ascertain the chemical structure of the compounds.

*Synthesis of 3-(4-((4-(dodecyloxy)benzoyl)oxy)phenyl)acrylic acid (**1**)*

4-(dodecyloxy)benzoic acid (10 mol) was synthesized according to our earlier report [21] and then it was allowed to react with excess thionyl chloride (40 mol) in the presence of benzene at 85 °C for 5 h. The unreacted $SOCl_2$ and benzene were removed under vacuum to get 4-(dodecyloxy)benzoyl chloride for further use. 4-Hydroxycinnamic acid (4.88 g, 15 mol) was dissolved separately in dimethylsulphoxide (100 mL), water (100 mL) and sodium hydroxide (1.32 g, 34 mol). 4-(dodecyloxy)benzoyl chloride (2.47 g, 15 mol) was slowly added to each of the above mixtures at 0 °C with vigorous stirring. After the reaction was allowed to proceed for 2 h at room temperature, the reaction mixture was neutralized to pH 6–7 by using dilute hydrochloric acid. The solid intermediate which obtained while filtering was thoroughly washed with water. The product was vacuum dried and recrystallized in methanol to yield 3-(4-((4-(dodecyloxy)benzoyl)oxy)phenyl)acrylic acid **(1)** (4 g, yield: 68%, m.p:176–178 °C). $C_{42}H_{43}N_3O_5$: calcd C 75.31, H 6.47, N 6.27; found C 75.20, H 6.39, N 6.23. FT-IR (KBr pellet, cm^{-1}): 2880, 2972 (C—H stretch. aliphatic), 1725 (C═O, ester), 1630 (C═C stretch. vinyl group of cinnamate), 1607 (C═C str. of aromatic), 1140 (C—O str. of ester), 921 (C—H plane bending). ^1H NMR (400 MHz, $CHCl_3$) δ 10.64 (s, aromatic-COOH, 1H), 7.89–6.91 (d, aromatic-H, 8H), 7.39 (d, J = 13.6 Hz, olefinic-H, 1H), 6.56 (d, J = 13.6 Hz, olefinic-H, 1H), 3.91–3.86 (t, J = 6.8 Hz, —OCH_2, 2H), 1.72–0.81 (m, aliphatic-CH_2, 20H), 0.82–0.876 (s, aliphatic-CH_3, 3H). ^{13}C NMR (125 MHz, $CHCl_3$) δ: 13.6 (aliphatic-CH_3), 21.2–30.6 (aliphatic-CH_2), 67.8 (OCH_2), 113.6–163.5 (aromatic-carbon), 115.2, 143.4 (olefinic carbon) 164.1 (—C═O ester) 169.4 (—COOH).

*Synthesis of 4-((E)-3-(4-((E)-(4-cyanophenyl)diazenyl)phenoxy)-3-oxoprop-1-en-1-yl)phenyl 4-(dodecyloxy)benzoate (**4a**)*

A round bottomed flask containing 3-(4-((4-(dodecyloxy)benzoyl)oxy)phenyl)acrylic acid **(1)** (1.62 g, 3.5 mol), benzene (20 mL) and thionyl chloride (0.3 g, 4.2 mol) were held under nitrogen atmosphere. The reaction was carried out at 85 °C until transparent solution was obtained. After the reaction, the solvent and thionyl chloride were removed under vacuum, and the obtained product, 3-(4-((4-(dodecyloxy)benzoyl)oxy)phenyl)acrylic acid chloride **(2)**, was used without further purification for the next reaction. In a round bottomed flask, (E)-4-((4-hydroxyphenyl)diazenyl)benzonitrile **(3)** (1.49 g, 3.17 mol) was dissolved in 40 mL of THF, then triethylamine (0.38 g, 3.8 mol) was added

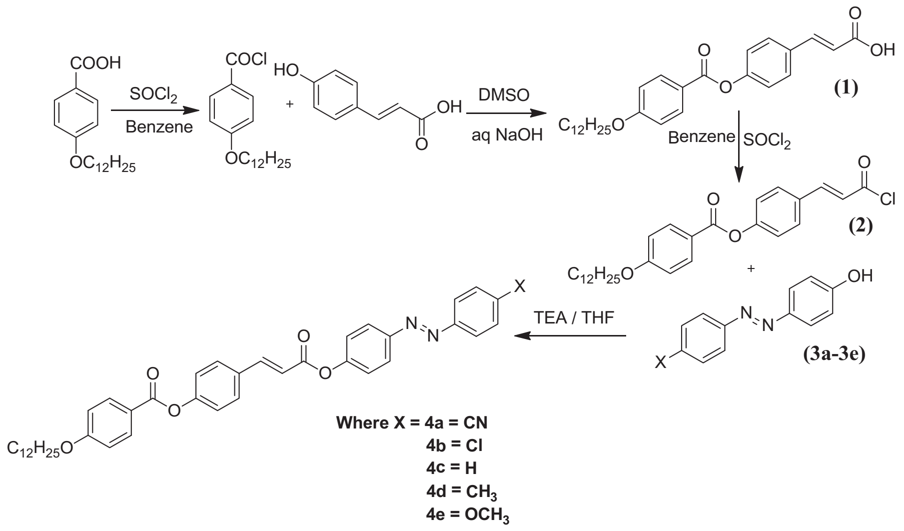

Scheme 1. Synthetic of liquid crystal compounds (**4a**–**4e**).

with agitation for 30 min. Afterwards 3-(4-((4-(dodecyloxy)benzoyl)oxy)phenyl)acrylic acid chloride **(2)** (0.7 g, 3.1 mol) in 25 mL of THF was added drop wise keeping the temperature in the range 0 to −5 °C. Temperature of the reaction mixture was allowed to rise slowly to room temperature and the content was stirred for 1 h. The quaternary ammonium salt thus formed was filtered and the solvent was evaporated in a rotary evaporator, the crude solid obtained was washed with petroleum-ether and purified by column chromatography (Yield: 65%). The similar procedure was adapted for the synthesis of other substituted compounds (**4b**–**4e**; Scheme 1). $C_{42}H_{43}N_3O_5$: calcd C 75.31, H 6.47, N 6.27; found C 75.20, H 6.39, N 6.23. FT-IR (KBr pellet, cm^{-1}): 2854, 2934 (C—H stretch. aliphatic), 1730 (C=O, ester), 1623 (C=C stretch. vinyl group of cinnamate), 1616 cm^{-1} (N=N), 1601 (C=C str. of Aromatic), 1160 (C—O str. of ester), 950 (C—H plane bending). ^1H NMR (400 MHz, $CHCl_3$) δ 8.30–6.94 (d, aromatic-H, 16H), 7.48 (d, J = 13.5 Hz, olefinic-H, 1H), 6.51 (d, J = 13.5 Hz, olefinic-H, 1H), 4.04–3.39 (t, J = 6.5 Hz, —OCH_2, 2H), 1.54–1.23 (m, aliphatic-CH_2, 20H), 0.93–0.90 (m, aliphatic CH_3, 3H).^{13}C NMR (125 MHz, $CHCl_3$) δ: 13.9 (aliphatic-CH_3), 21.8–31.4 (aliphatic-CH_2), 68.3(OCH_2), 113.6–154.2 (aromatic carbon), 115.9, 146.9 (olefinic carbon) 117.3 (aromatic-CN), 164.7 (—C=O ester).

*4-((E)-3-(4-((E)-(4-chlorophenyl)diazenyl)phenoxy)-3-oxoprop-1-en-1-yl)phenyl 4-(dodecyloxy)benzoate (**4b**)*

$C_{41}H_{43}N_2O_5$: Yield: 60%. calcd C 72.60, H 6.39, N 4.13; found C 72.10, H 6.26, N 4.02. FT-IR (KBr pellet, cm^{-1}): 2864, 2942 (C—H stretch. aliphatic), 1723 (C=O, ester), 1618 (C=C stretch. vinyl group of cinnamate), 1611 cm^{-1} (N=N), 1587 (C=C str. of aromatic), 1154 (C—O str. of ester), 955 (C—H plane bending). ^1H NMR (400 MHz, $CHCl_3$) δ 8.25–6.95 (d, aromatic-H, 16H), 7.49 (d, J = 13.3 Hz, olefinic-H, 1H), 6.52 (d, J = 13.3 Hz, olefinic-H, 1H), 4.07–4.03 (t, J = 6.6 Hz, —OCH_2, 2H), 1.64–1.26 (m, aliphatic CH_2, 20H), 0.89–0.84 (s, aliphatic CH_3, 3H).^{13}C NMR (125 MHz, $CHCl_3$) δ: 13.6 (aliphatic CH_3), 21.4–31.4 (aliphatic-CH_2), 67.7 (OCH_2), 112.5–152.3 (aromatic carbon), 113.8, 147.5 (olefinic carbon), 163.5 (—C=O ester).

*4-((E)-3-oxo-3-(4-((E)-phenyldiazenyl)phenoxy)prop-1-en-1-yl)phenyl 4-(dodecyloxy)benzoate (**4c**)*

$C_{41}H_{44}N_2O_5$: Yield: 71%. calcd C 76.37, H 6.87, N 4.34; found C 76.02, H 6.29, N 4.27. FT-IR (KBr pellet, cm^{-1}): 2872, 2936 (C—H stretch. aliphatic), 1726 (C=O, ester), 1610 (C=C stretch. vinyl group of cinnamate), 1601 cm^{-1} (N=N), 1605 (C=C str. of aromatic), 1152 (C—O str. of ester), 953 (C—H plane bending). ^1H NMR (400 MHz, $CHCl_3$) δ 8.38–6.99 (d, aromatic-H, 17H), 7.50 (d, *J* = 13.4 Hz, olefinic-H, 1H), 6.49 (d, *J* = 13.4 Hz, olefinic-H, 1H), 4.04–4.01 (t, *J* = 6.8 Hz, OCH_2, 2H), 1.60–1.29 (m, aliphatic CH_2, 20H), 0.80–0.72 (s, aliphatic CH_3, 3H). ^{13}C NMR (125 MHz, $CHCl_3$) δ: 13.8 (aliphatic CH_3), 21.5–30.6 (aliphatic-CH_2), 67.8 (OCH_2), 112.3–152.9 (aromatic carbon), 113.7, 147.7 (olefinic carbon), 163.3 (—C=O ester).

*4-((E)-3-oxo-3-(4-((E)-p-tolyldiazenyl)phenoxy)prop-1-en-1-yl)phenyl 4-(dodecyloxy)benzoate (**4d**)*

$C_{42}H_{46}N_2O_5$: Yield: 59%. calcd C 76.56, H 7.03, N 4.25; found C 76.17, H 6.96, N 4.05. FT-IR (KBr pellet, cm^{-1}): 2848, 2911 (C—H stretch. aliphatic), 1733 (C=O, ester), 1621 (C=C stretch. vinyl group of cinnamate), 1612 cm^{-1} (N=N), 1606 (C=C str. of aromatic), 1164 (C—O str. of ester), 925 (C—H plane bending).^1H NMR (125 MHz, $CHCl_3$) δ 8.40–6.99 (d, aromatic-H, 16H), 7.51 (d, *J* = 13.4 Hz, olefinic-H, 1H), 6.53 (d, *J* = 13.4 Hz, olefinic-H, 1H), 4.08–4.03 (t, *J* = 6.4 Hz, OCH_2, 2H), 2.45–2.38 (s, aromatic-CH_3, 3H), 1.51–1.29 (m, aliphatic-CH_2, 20H), 0.91–0.90 (s, aliphatic-CH_3, 3H).^{13}C NMR (125 MHz, $CHCl_3$) δ: 13.0 (aliphatic-CH_3), 20.4–21.6 (aromatic-CH_3) 25.0–30.9 (aliphatic-CH_2), 67.3 (OCH_2), 111.0–151.9 (s, aromatic carbon), 113.3, 149.2 (olefinic carbon), 163.9 (—C=O ester) (see Fig. 3).

*4-((E)-3-(4-((E)-(4-methoxyphenyl)diazenyl)phenoxy)-3-oxoprop-1-en-1-yl)phenyl 4-(dodecyloxy)benzoate (**4e**)*

$C_{42}H_{46}N_2O_6$: Yield: 75%. calcd C 74.75, H 6.87, N 4.15; found C 74.14, H 6.58, N 4.14. FT-IR (KBr pellet, cm^{-1}): 2851, 2957 (C—H stretch. aliphatic), 1724 (C=O, ester), 1617 (C=C stretch. vinyl group of cinnamate), 1597 cm^{-1} (N=N), 1616 (C=C str. of Aromatic), 1150 (C—O str. of ester), 951 (C—H plane bending). ^1H NMR (400 MHz, $CHCl_3$) δ 8.34–6.95 (d, aromatic-H, 16H), 7.48 (d, J = 13.5 Hz, olefinic-H, 1H), 6.46 (d, J = 13.5 Hz, olefinic-H, 1H), 4.03–3.99 (t, J = 6.8 Hz, —OCH_2, 2H), 3.87 (s, aroamtic-OCH_3, 3H), 1.62–1.24 (m, aliphatic-CH_2, 20H), 0.92–0.90 (s, aliphatic-CH_3, 3H).^{13}C NMR (125 MHz, $CHCl_3$) δ: 13.4 (aliphatic CH_3), 21.8–30.3 (aliphatic CH_2), 54.8 (aromatic-OCH_3), 67.9 (OCH_2), 112.3–152.3 (aromatic carbon), 113.6, 147.9, (olefinic carbon), 164.6 (—C=O ester).

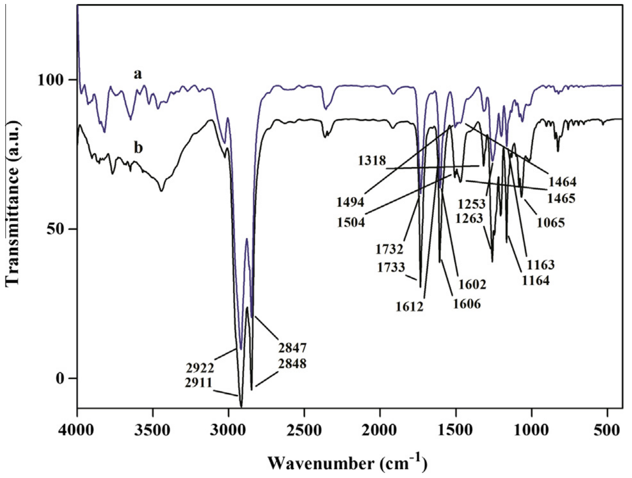

Fig. 1. (a) Before irradiation of compound **4d**. (b) After irradiation of compound **4d**.

Results and discussion

Compounds **4a**–**4e** was synthesized following very simple methods by using standard procedures as described in Scheme 1. The empirical composition and the molecular structures of all the final compounds were confirmed by elemental analysis and spectral techniques respectively. The analytical data are in good agreement with their chemical structures. All compounds in series **4a**–**4e** exhibited IR absorption peak intensity between 2957 and 2848 cm^{-1} which are characteristic of asymmetric C—H stretching and symmetric C—H stretching respectively. Moreover, other peaks observed at 1733–1724 cm^{-1} (C=O stretching), 1610–1623 cm^{-1} (—C=C— Str. vinyl group of cinnamate), 1616–1597 cm^{-1} (N=N), 1263–1065 cm^{-1} (C—O—C Str. of alkoxy), 1164–1150 cm^{-1} (C—O Str. of ester) which confirms the presence of carbonyl group and the formation of ester linkage between azobenzene unit and cinnamoyl unit respectively.

The rod like shape of four ring molecules possesses a dodecyloxy chain attached at one end of the molecule whereas other end occupying different terminal substituents. The CN group at the end of the terminal position will increase the polarity and induce the overall polarizability of the compounds. The highly polarizable aromatic ester involves in conjugative interaction and vinyl ester involves in mesomeric interaction within the molecule. Moreover, Compounds containing unsaturated bonds such as azo, olefinic unit are frequently employed since they restrict the freedom of rotation. Such groups could conjugate with benzene rings, enhancing the anisotropic polarizability. This increases the molecular length and maintains rigidity. The two neighbouring molecule with a strong polar (CN) moiety at one end arrange to assemble the antiparallel orientation, which results in overlapping of the molecule. This brings about strongest attraction between them leading to high clearing transition temperatures and thermal stability compared to other terminally substituted compounds. This rod shaped molecules induces layer ordering which is aided by strongly polar end substituents, enhancing terminal attraction that is sufficiently enough to promote the formation of smectic phases.

POM and DSC studies

In order to explore the influence of the central linkage and terminal substitution on the mesophase behaviour of the liquid crystalline compounds, these were characterized and studied by differential scanning calorimetry (DSC) and polarising optical microscope (POM). Phase transition temperature and associated enthalpy changes of the synthesized compounds are given in Table 1. The mesophase assignments resulting from POM observation are in good accordance with the corresponding DSC thermograms. The liquid crystalline textures of the compounds **(4a–4e)** were observed on hot stage optical polarized microscope in the range of 30–210 °C upon heating and cooling cycles at 10× magnification. All compounds displayed a clear cut transition temperature in the DSC thermograms (Fig. 5). The recognition of nematic and smectic phases was initially performed on the basis of POM textures observation. Upon heating and cooling compound **4a** exhibits two transition peaks, in which the transitions from crystal to SmA and SmA to isotropic occurs while heating to 180 °C and the reverse transitions occur on cooling to 150 °C, respectively as shown in Fig. 6.

Likewise, compound **4b** also exhibits two transition peaks on heating corresponding to crystal – nematic and nematic – isotropic transitions. The heating transitions displayed schlieren texture of

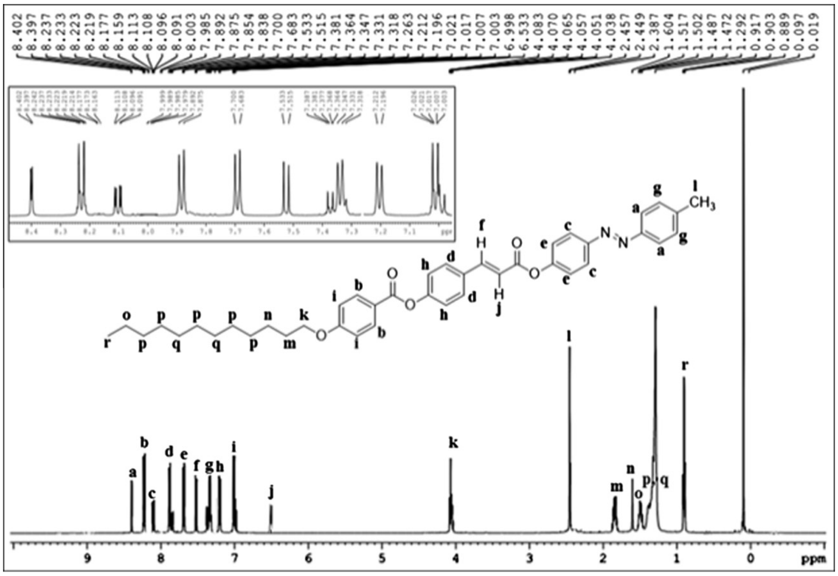

Fig. 2. ^{1}H NMR spectrum of compound **4d**.

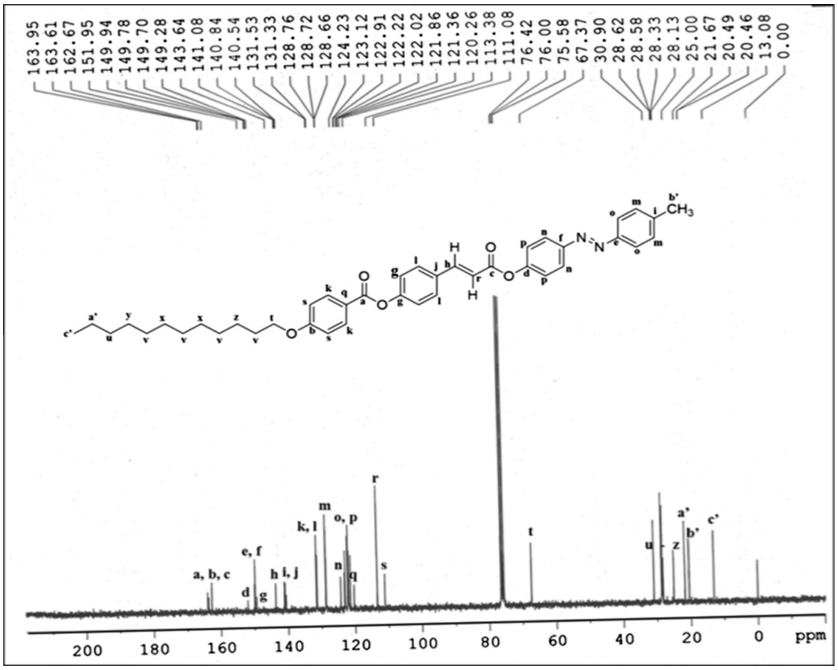

Fig. 3. ^{13}C NMR spectrum of compound **4d**.

Table 1
Phase transition temperatures (°C) and enthalpies (kJ mol^{-1}, in parentheses) of **4a**–**4e** on the heating and cooling runs at a scan rate of 5 °C min^{-1}.

Compound	Scan	Phase transitions (°C) (enthalpy changes, J g^{-1})
4a	Heat	Cr 101 (6.8) SmA 195 (12.7) I
	Cool	I 193 (21.5) SmA 74 (−65.7) Cr
4b	Heat	Cr 133 (6.9) SmA 187 (23.7) N 214 (13.4) I
	Cool	I 212 (24.4) N 136 (23.4) SmA 68 (−6.2) Cr
4c	Heat	Cr 95 (0.06) N 114 (18.5) I
	Cool	I 112(20.8) N 94 (−0.83) SmA 78 (−67.06) Cr
4d	Heat	Cr 87 (14.0) SmA 93 (22.4) N 98 (14.7) I
	Cool	I 97(21.8) N 88 (23.2) SmA 84 (−30.04) Cr
4e	Heat	Cr 96 (15.3) SmA 108 (8.8) N 128 (1.9) I
	Cool	I 126 (0.9) N 107 (1.2) SmA 74 (23.6) Cr

Transition temperatures (°C) and enthalpies (in parentheses, J g^{-1}) were measured by DSC (at a heating and cooling rates of 5 °C min^{-1}). Cr = Crystalline phase; SmA = smectic A phase; N = Nematic phase; I = Isotropic liquid.

nematic phase with fourfold brush at 200 °C. Whereas, three transition peaks were observed on cooling, which corresponds to isotropic–nematic, nematic – SmA and SmA – crystal transitions, displaying schlieren nematic at 210 °C and SmA phase at 136 °C.

DSC of compound **4c** displayed a single peak on first heating which exhibits a nematic phase and two peaks were observed on first cooling due to SmA and crystal as shown in Fig. 5. On second heating and cooling, the compound **4c** showed mesophase behaviour in DSC (Fig. 5). But microscope revealed three phases on cooling which corresponds to isotropic – nematic, nematic – smectic A and smectic A – crystal transition for compound **4c** as shown in Fig. 6. While heating to isotropic liquid, the compound **4c** exhibited schlieren nematic phase at 100 °C and on cooling from isotropic liquid, it displayed nematic at 104 °C and SmA texture at 93 °C. Similarly, the compounds **4d** and **4e** exhibited enantiotropic behaviour. The compound **4d** exhibited schlieren nematic phase between 94 and 98 °C on heating and SmA mesophase on cooling between 88 and 93 °C. The compound **4e** exhibited schlieren texture of nematic phase for heating at 110 to 124 °C and fan shaped textures of SmA phase for cooling at 107–80 °C. Compounds **4d** and **4e** exhibited same behaviour as that of **4b**. In comparison, **4a** and **4b** exhibited broader transition temperature range than **4d** and **4e** indicating that the electron withdrawing terminal substituent CN and Cl moiety possessing strong π–π* interaction enhanced the head to tail molecular interaction. All compounds revealed enantiotropic mesomorphism. Both the compounds **4a** and **4b** having higher homologues of electron withdrawing substituent in terminal azobenzene containing cyano and chloro group were found to exhibit smectic A to isotropic transition at 195 °C and nematic to isotropic transition at 214 °C, respectively. Whereas compounds **4d** and **4e** having higher homologues of electron donating substituent in terminal azobenzene having methyl and methoxy substituent exhibits nematic to isotropic transition at 98 °C and at 128 °C, respectively.

The results revealed that the rigidity of the mesogenic core, flexible spacer length and types of terminal substituents has large influence on intermolecular and diploe induced dipole interactions. The size and polarity nature of the terminal substituent is important as it depends on the variation in phase transition temperature. The N–I (nematic–isotropic) thermal stability of compounds **4a** and **4b** are higher than **4d** and **4e**. This is because benzene ring with —CN and —Cl groups in terminal position will endow the molecule with a higher polarity, high thermal attraction and hence higher N–I thermal stability. It is well known that the stability of the mesophase would be extended by an increase in the polarity or polarizability of the mesogenic part of the molecule. This is due to increase the nematic and smectic thermal stabilities because of the resulting increase in lateral attractions. The relative strength of the lateral and terminal cohesive forces between molecules a type of the mesophase formed. The weak terminal intermolecular cohesions and strong lateral attraction will give rise to a smectic mesophase. The compounds **4a**–**4e** differs only in terminal substituent but has same central linkage, a cinnamoyloxy (—CH═CH—COO—) group which is connected with alkyloxyphenylester (—COO—) group. The presence of this double bond system (cinnamoyloxy group) increases the length of polarizability of rod like molecules and enhances the thermal stability. All the

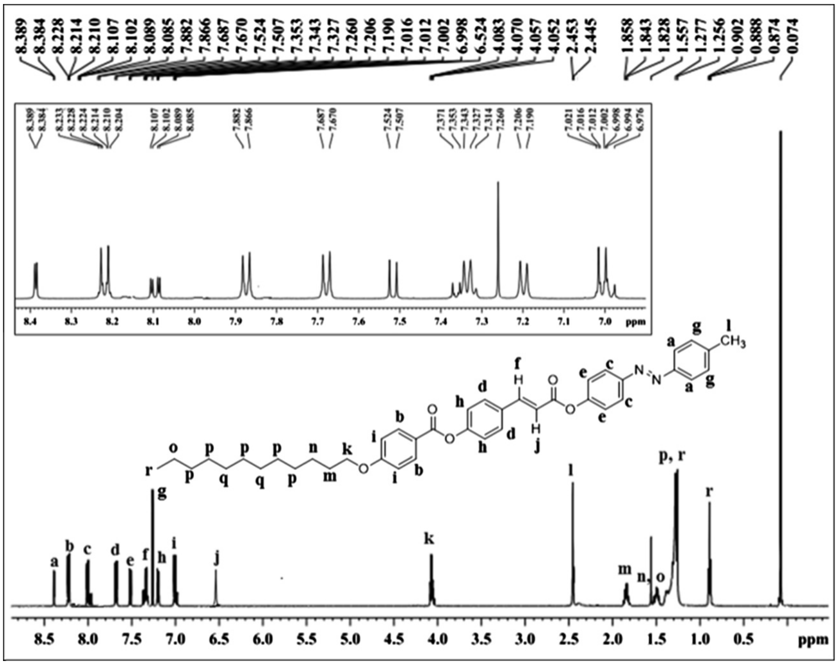

Fig. 4. ^{1}H spectrum of after irradiation of compound **4d**.

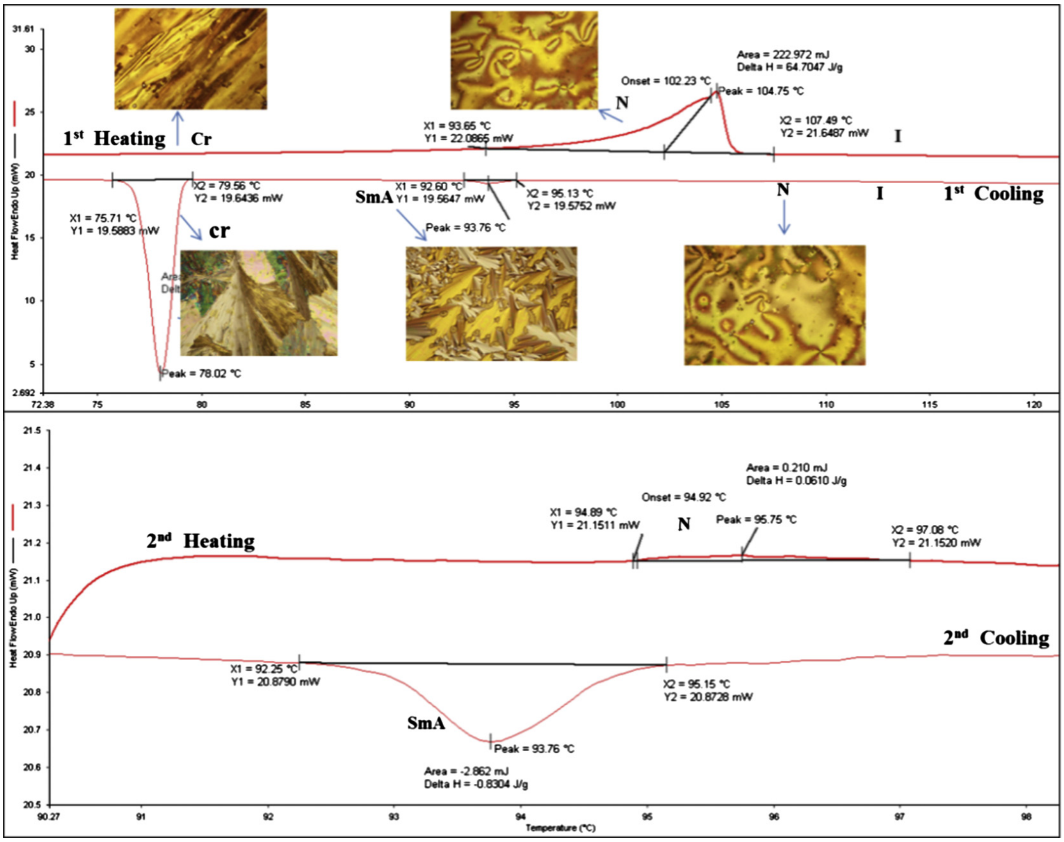

Fig. 5. DSC thermograms of compound **4c** recorded at a rate of 5 °C/min.

above factors determine the type of mesomorphism and physical properties of these compounds (see Fig. 7).

The compound **4d** was found to be soluble in chloroform both before and after irradiation with UV light for 2 h after evaporating the solvents. The irradiated sample was further subjected for FT-IR, ^{1}H NMR, POM and DSC analysis. On comparing the FT-IR spectra (Fig. 1(a) and (b)) before and after UV exposure **(4d)**, it was found that there is no change in the intensity of the absorption band of the olefinic double bond stretching vibration at 1607 cm^{-1} since it does not undergo any crosslinking but only cis–trans

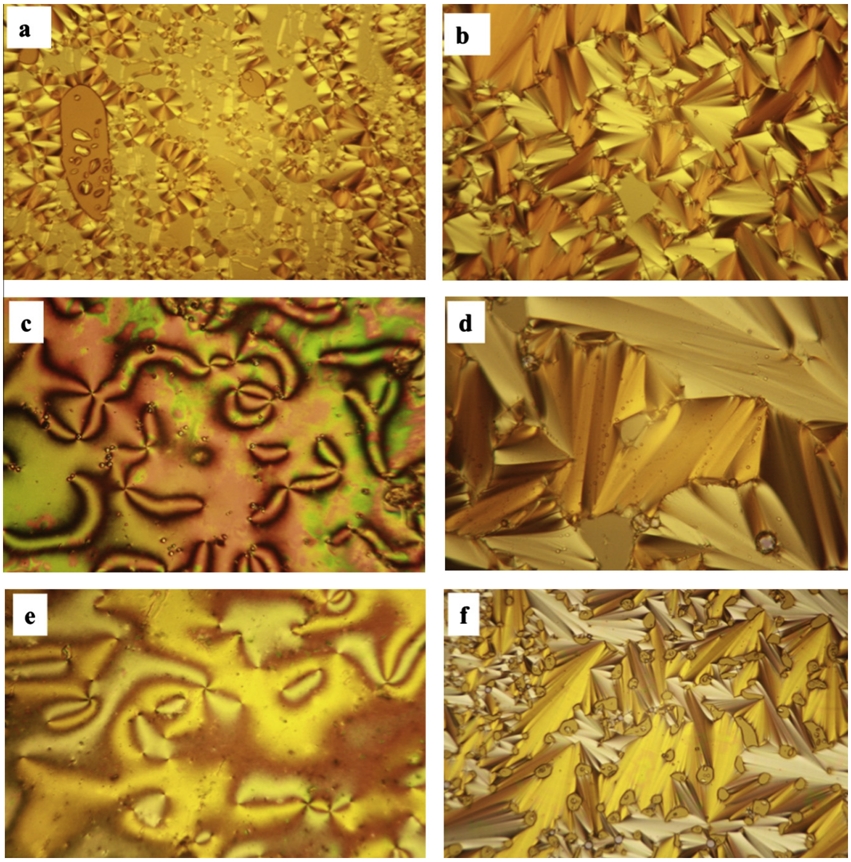

Fig. 6. Optical photomicrographs for compounds **4a**–**4c** liquid crystal phases upon heating and cooling: (a and b) **4a** exhibits SmA phase at 180 °C and 150 °C (c and d) **4b** displays schlieren texture of nematic phase at 200 °C and fan shaped SmA phase at 130 °C (e) and (f) **4c** shows schlieren texture of nematic phase at 100 °C and focal conical fan shaped SmA at 85 °C respectively. All the optical micrographs were taken with a magnification of 10×.

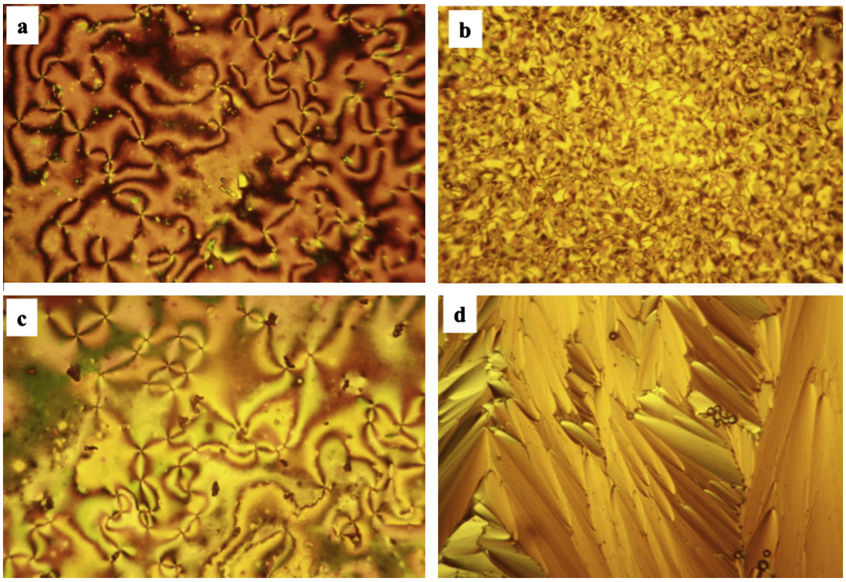

Fig. 7. Microphotographs of the compounds **4d** and **4e** liquid crystal phase upon heating and cooling: (a and b) **4d** exhibits schlieren texture of nematic phase at 98 °C and SmA phase at 88 °C (c and d) **4e** displays schlieren texture of nematic phase 124 °C and fan shaped texture of SmA phase at 104 °C.

isomerization of olefinic unit in cinnamate and azo group occurs. Further analysis with ^{1}H NMR spectrum (Fig. 4) of compound **4d** after UV irradiation was carried out in order to understand the isomerization behaviour of this compound. The spectrum after irradiation indicated some changes. In Fig. 2 in trans-isomer the olefinic proton (f) shows doublet whereas in Fig. 4 the corresponding cis isomer the olefinic proton (f) exhibits multiplet. Further, the absence of proton signal at 3.8 ppm clearly indicated that the

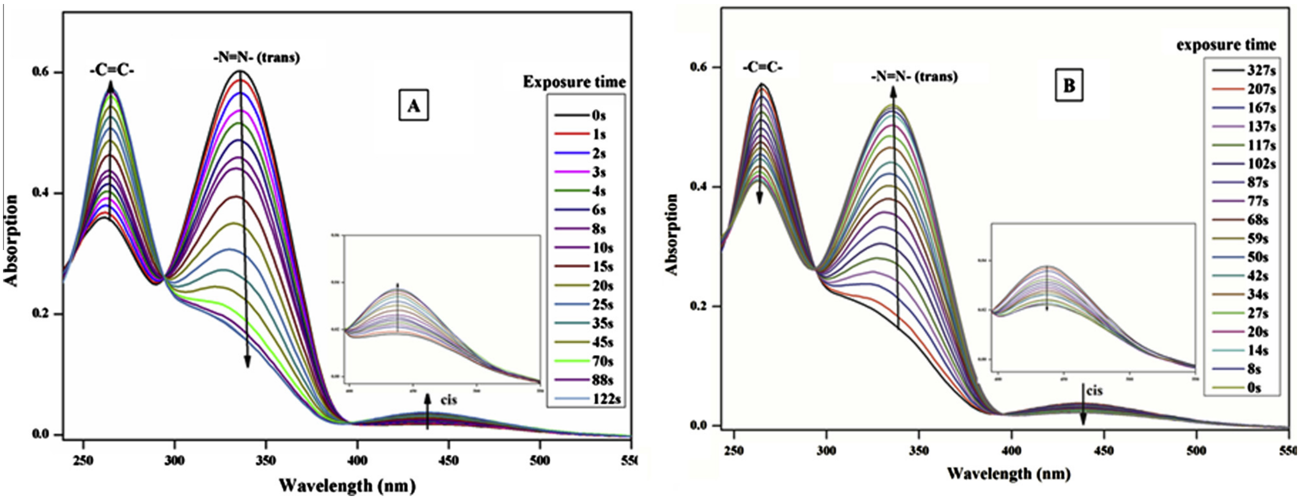

Fig. 8. Absorption spectrum of 4a (A → trans–cis isomerization upon UV light and B → cis–trans isomerization (reversible isomerization) upon visible light.

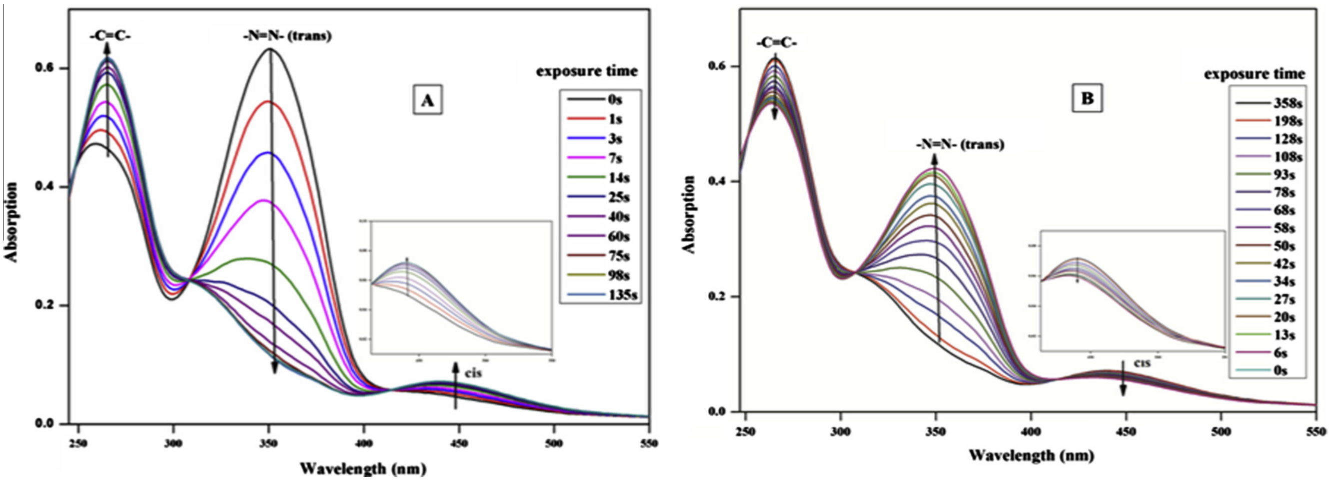

Fig. 9. Absorption spectrum of **4b** (A → trans–cis isomerization upon UV light and B → cis–trans isomerization (reversible isomerization) upon visible light.

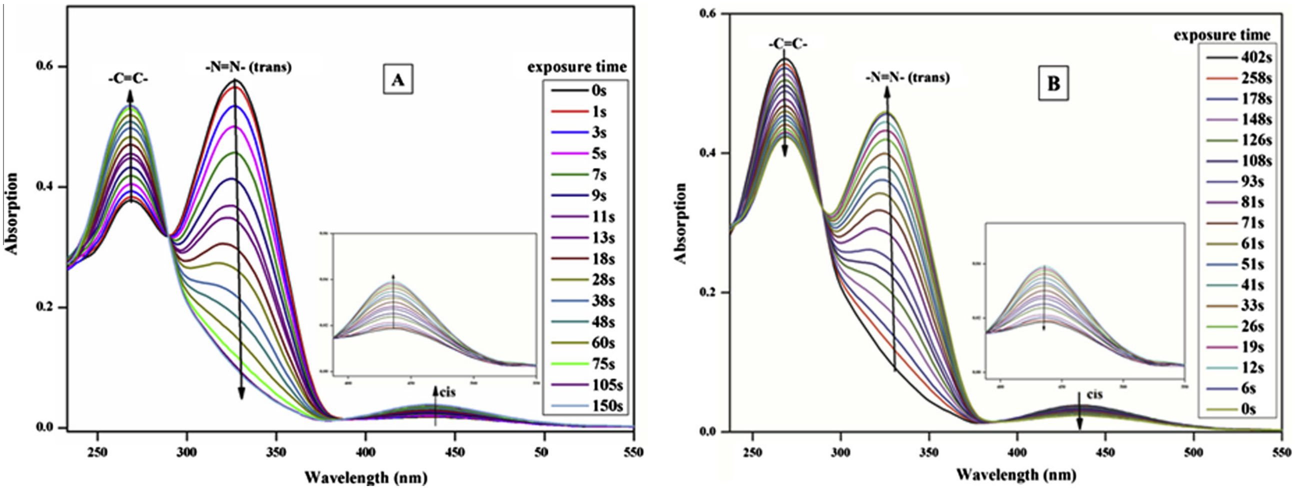

Fig. 10. Absorption spectrum of **4c** (A → trans–cis isomerization upon UV light and B → cis–trans isomerization (reversible isomerization) upon visible light.

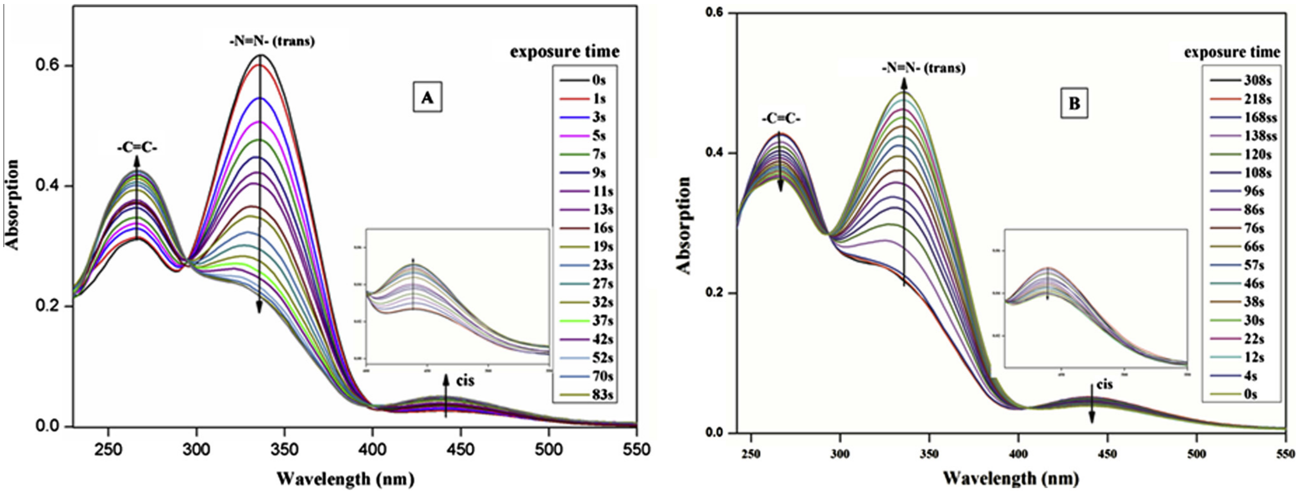

Fig. 11. Absorption spectrum of **4d** (A → trans–cis isomerization upon UV light and B → cis–trans isomerization (reversible isomerization) upon visible light.

compound **4d** does not undergo photocrosslinking reaction, but undergo only trans–cis–trans isomerization of azo and olefinic groups. Similar behaviour was found for the other four compounds.

We were interested to study the photochemical properties of organic compounds **4a**–**4e**. Accordingly, we have prepared these compounds with azo and cinnamic acid functional moieties. UV-spectroscopy studies indicated that the absence of photocrosslinking also gave an evidence for the occurrence of photoisomerization. The absence of photocrosslinking could be attributed to the azo group that is highly photoreactivity than the other functional groups. Before UV irradiation, the initial phase of compound **4d** exhibits schlieren nematic, in which the azobenzene was in the trans-form; From POM analysis after UV irradiation, nematic phases could be observed, where the azobenzene transforms to cis form. It is found that these compounds exhibit liquid crystal properties with slight decrease in transition temperatures. So it changes from order to disorder transition. It was indicated that the Tg (glass transition temperature) of the compound **4d** slightly decreased after irradiation. The POM analysis of the compound **4d** after irradiation found to exhibit nematic to isotropic phase at 96 °C and isotropic from nematic phase at 87 °C, and crystallised at 81 °C. As well as the compound **4d** exhibited liquid crystalline property and this is attributed to the restricted molecular mobility in the backbone.

Photochemical properties

In order to investigate the photoisomerization behaviour, the terminal substituted azobenzene compounds **4a**–**4e** was irradiated with UV–visible (365 and 420 nm) light. As shown in Figs. 8(A)–12(A) the band corresponding to π–π* and n–π* decreases with increase in the irradiation time. In Figs. 8(B)–12(B), the band corresponding to the isomerized product increases by increasing the irradiation time. This confirmed that the photoisomerization has occurred in the range of 365–420 nm. The photoisomerization process of substituted azobenzene moieties and their absorption data were summarized in Table 2. From the UV irradiation studies, we have observed that there is no cause of photodegradation process taken place in case of compounds having photochromic moieties like cinnamate and azo segment. These compounds were observed with photoisomerization taken with different time intervals which depend upon terminal substituents. These compounds exhibit strong UV–visible absorption band around 325–380 nm, which is attributed to π–π* transition of the trans-isomer and a

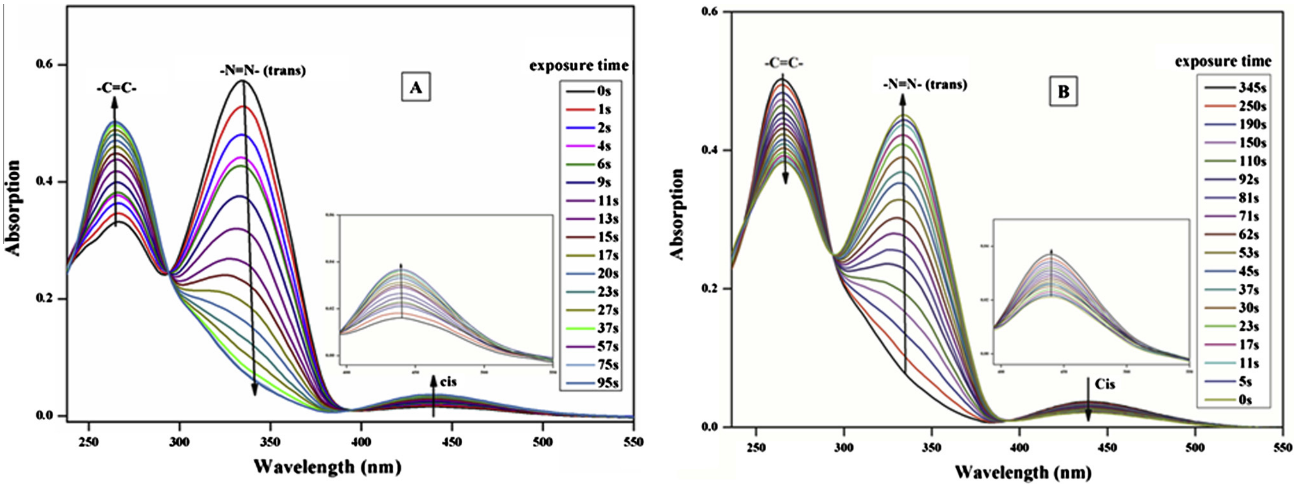

Fig. 12. Absorption spectrum of **4e** (A → trans–cis isomerization upon UV light and B → cis–trans isomerization (reversible isomerization) upon visible light.

Table 2
Photoisomerization of compounds **4a**–**4e**.

Compound	λ_{max}[a] (nm)	λ_{max}[b] (nm)	λ_{max}[c] (nm)	Isobestic point[d] (nm)	T_{365}[e] (s)	T_{420}[f] (s)
4a (CN)	263	335	435	294, 396	122	327
4b (Cl)	264	350	440	308, 415	135	358
4c (H)	266	326	433	292, 385	150	402
4d (CH_3)	264	336	439	295, 401	83	338
4e (OCH_3)	264	335	439	294, 393	95	308

[a,b] Maximum absorption involved in trans–cis isomerization due to π–π* transition of compounds in $CHCl_3$ solution; concentration 1×10^{-5}.

[c] Maximum absorption involved in cis–trans isomerization due to in n–π* transition.

[d] Isobestic points (nm) in absorption during UV/visible irradiation (365/420 nm).

[e] Time reached the photostationary state of trans–cis photoisomerization.

[f] Time reached the photostationary state of cis–trans (reversible) photoisomerization.

weak absorption band was also found in the range of 390–460 nm, due to n–π* transition of the cis isomer.

The compound **4a** irradiated at 365 nm (Fig. 8(A)), caused the trans–cis (E–Z) isomerization, resulting with a dramatic decrease in the absorption band from 335 nm and the absorbance band at 435 nm was gradually increased by reaching a photostationary state after 122 s and thereafter, there is no any significant change in the spectra. Isobestic points of **4a** were observed at 294 and 396 nm, corresponding to trans–cis photoisomerization as these suggesting that only two isomers (E and Z isomers) could exist. Simultaneously, a reversible photoisomerization was also studied for the compound **4a**. The UV irradiated compound **4a** was further irradiated for 2 h using the visible light in the same concentration of chloroform solution at room temperature. The transformed cis form of the azobenzene group from the trans-form was ensured from the increasing absorption band at 335 nm and also from the dramatic decrease in the absorption band at 435 nm. The photostationary state reached at 327 s, which was induced by the cis–trans (reversible) isomerization process as seen in Fig. 8(B). Similar results were observed for all the remaining terminal substituted compounds **(4b–4e)** which might be resulted from the geometric change of trans–cis and cis–trans isomer of the azo compounds and vice versa, as shown in Fig. 9–12. The compounds **4a**–**4e** does not undergo photocrosslinking reaction in the UV–visible region because of α, β-unsaturated keto group only isomerizes to enol form. This forbids the photocrosslinking reaction. Further the photosensitive compounds were repelling each other due to the steric hindrance between the molecules as shown in Fig. 13.

The compound **4b** exhibits an absorption shifted to 350 nm, in the UV–visible region which is attributed to the π–π* transition of the trans-isomer. The reason is due to an increase in electron density of the system due to high electronegative chloro substituents, which cause a red shift when compared to other substituents. Another band at 440 nm arises due to n–π* transitions of the cis isomer. The time taken for total isomerization process depends upon the nature of the terminal substituents. As the compounds **4a** and **4b** have electron withdrawing groups, their photoisomerization process takes longer time when compared to electron donating groups (**4d** and **4e**). The mesomeric and resonance effect were altered by the nature of the electron withdrawing/donating groups in the compound. The effect of substituents at the para positions decreases the time of photoisomerization of the compound are given in the order of H > Cl > CN > OCH_3 > CH_3.

Conclusion

We have synthesized and characterized five terminally substituted azobenzene chromophores with mesomorphic nature having azocinnamate as central linkages and with different terminal groups. The compounds exhibited nematic, smectic mesophase behaviour due to the cohesive forces acting between the molecules which were studied by DSC and POM. The effect of terminal substituents, central linkage (—CH=CH—COO), azobenzene and the spacer attached also plays a crucial role in the formation of the mesophase. The rigidity of the mesogenic core, flexible spacer length and different terminal substituents has large influence on intermolecular and dipole induced dipole interaction. Also in these compounds the presence of olefinic double bond system increases the length of polarizability of rod like molecules and enhances the thermal stability. These above factors determine the type of mesomorphism. This compounds exhibit photoisomerization process which depends on the different substituents attached to the terminal azobenzene and the time period taken for the process is also illustrated.

Acknowledgements

P.K. gratefully acknowledges the University Grants Commission, New Delhi, Government of India [39-691/2010 (SR)] for the financial support. Instrumentation facility provided under FIST-DST and DRS-UGC to department of chemistry, Anna University were sincerely acknowledged.

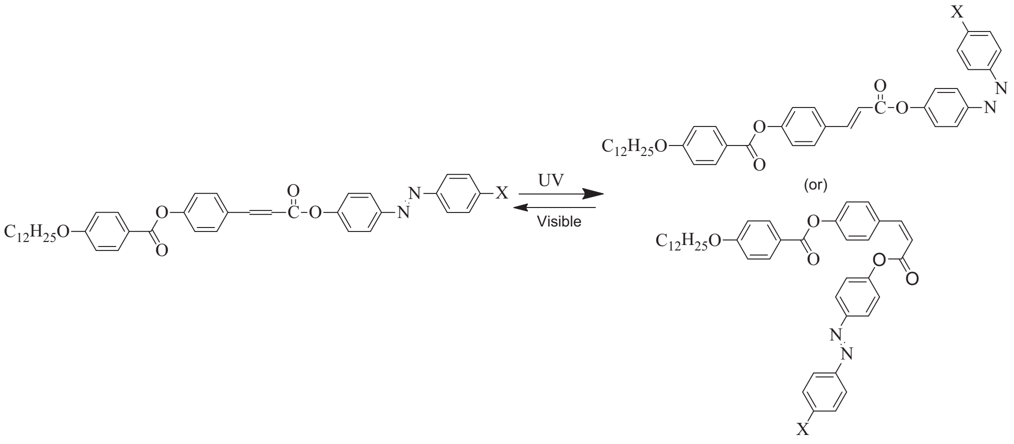

Fig. 13. Photoisomerization of target molecule under UV/visible light.

References

[1] D. Demus, J. Goodby, G.W. Gray, H.W. Spiess, W. Vill, Handbook of Liquid Crystals, Wiley-VCH, Weinheim, 1998.
[2] R.W. Date, C.T. Imrie, G.R. Luckhurst, J.M. Seddon, Liq. Cryst. 12 (1992) 203.
[3] B.T. Thaker, J.B. Kanojiya, Liq. Cryst. 38 (2011) 1035.
[4] T. Ikeda, T. Sasaki, K. Ichimura, J. Am. Chem. Soc. 116 (1994) 625.
[5] N. Boden, R.C. Borner, R.J. Bushby, A.N. Cammidge, M.V. Jesudason, Liq. Cryst. 15 (1993) 851.
[6] A. Stracke, J.H. Wendorff, D. Goldmann, D. Janietz, Liq. Cryst. 27 (2000) 1049.
[7] G. Wang, M. Li, M. Yu, C. Guo, X. Chen, G. Li, E. Zhou, Liq. Cryst. 27 (2000) 867.
[8] I. Levesque, M. Lecerc, Macromolecules 30 (1997) 4347.
[9] E. Schab-Balcerzak, A. Sobolewska, A. Miniewicz, J. Jurusik. Poly. Eng. Sci. 48 (2008) 1755.
[10] E. Schab-Balcerzak, M. Siwy, M. Kawalec, A. Sobolewska, A. Chamera, A. Miniewicz, J. Phys. Chem. A. 113 (2009) 8765.
[11] X. Jiang, X. Chen, X. Yue, J. Zhang, S. Guan, H. Zhang, W. Zhang, Q. Chen, React. Funct. Poly. 70 (2010) 616.
[12] N. Tamai, H. Miyasaka, Chem. Rev. 100 (2000) 1875.
[13] Po-Chih Yang, Lu Ya-Ling, Chung-Yuan Li, J. Mol. Struc. 1015 (2012) 129.
[14] K. Rameshbabu, P. Kannan, R. Velu, P. Ramamurthy, Liq. Cryst. 32 (2005) 823.
[15] J.S. Dave, M. Menon, Bull. Mater. Sci. 23 (2000) 237.
[16] R.A. Vora, S.J. Rajput, Mol. Cryst. Liq. Cryst. 209 (1991) 265.
[17] G. Hegde, R.A. Alla, A. Matharu, L. Komitov, J. Mater. Chem. C. 1 (2013) 3600.
[18] Po-Chih Yang, Chung-Yuan Li, Wu Hung, Jen-Chieh Chiang, J. Taiwan Inst. Chem. Eng. 43 (2012) 480.
[19] Trirup Dutta Choudhury, Yongqiang Shen, Nandiraju V.S. Rao, Noel A. Clark, J. Organomet. Chem. 712 (2012) 20.
[20] M. Vijay Srinivasan, P. Kannan, A. Roy, J. Mater. Sci. 48 (2013) 2433.
[21] M. Vijaysrinivasan, P. Kannan, A. Roy, Liq. Cryst. 39 (2012) 1465.